Chapter 11
Photo-activated Cancer Therapy: Potential for Treatment of Brain Tumors

Henry Hirschberg

11.1 Introduction

The resistance of high grade glioma (glioblastoma multiforme; GBM) to therapeutic intervention is due to a number of factors. Among the most important are significant genetic variations, including numerous deletions, amplifications, and point mutations to receptor and suppressor genes. Additionally, the diffuse and infiltrative nature of GBMs makes complete surgical resection virtually impossible. The propensity of glioma cells to migrate along white matter tracts makes it clear that a cure is only possible if the migratory cells can be eradicated. Despite the factors already mentioned, 80% of GBMs recur within 2 cm of the resection margin, and therefore a reasonable starting point for improving the prognosis of GBM patients would be the development of improved local therapies capable of eradicating glioma cells in the margin, or brain-adjacent-to-tumor (BAT). Complicating successful therapy further are variations in blood–brain barrier (BBB) patency throughout the tumor and BAT volume—it is intact in some regions, while leaky in others and this has significant implications for the delivery of therapeutic agents. The BBB controls the passage of blood-borne agents into the central nervous system (CNS) and, as such, it plays a vital role in protecting the brain against pathogens. Although this protective mechanism is essential for normal brain function, it also poses a significant hindrance to the entry of drugs into the brain. The protective function of the BBB is particularly problematic for the treatment of infiltrating gliomas. Although surgery is used to remove gross tumor, standard adjuvant therapies consisting of radiation and chemotherapy often fail to eliminate infiltrating glioma cells in or beyond the BAT region—a zone that commonly extends several centimeters from the resection margin [1]. Infiltrating tumor cells are supplied with nutrients and oxygen by the normal brain

H. Hirschberg (✉)
Beckman Laser Institute, University of California, Irvine, CA, USA
e-mail: hhirschb@uci.edu

S.J. Madsen (ed.), *Optical Methods and Instrumentation in Brain Imaging and Therapy*, Bioanalysis: Advanced Materials, Methods, and Devices 3,
DOI 10.1007/978-1-4614-4978-2_11,

vasculature and consequently, protected by the BBB: few anti-cancer drugs are capable of crossing this barrier. The efficacy of any drug treatment depends on the ability of the therapeutic agent to reach its target. Therefore, destruction of infiltrating tumor cells is a crucial step for curing malignant gliomas. This cannot be accomplished until methods are developed to: (1) deliver drugs or carriers across the BBB at a selected site, or (2) selectively disrupt in a site-specific manner this protective barrier. Eradication of gliomas is highly unlikely without addressing the problems posed by the BBB. Although a number of therapeutic strategies have been attempted, the most popular include the local delivery of: (1) chemotherapeutic agents using polymer wafers, and (2) ionizing radiation in the form of brachytherapy [2, 3]. Unfortunately, neither of these strategies has resulted in significant prolongation of survival.

One potential method to improve drug delivery would therefore be to induce increased vascular permeability to these agents in the local tumor environment. Photodynamic therapy (PDT) is a treatment modality combining a photosensitizing drug and light to activate the photosensitizer in an oxygen-dependent manner resulting in oxidation of biomolecules in the light-exposed region. Details of the mechanism and effects of PDT have been covered in Chap. 9.

PDT has been traditionally used to destroy tumor cells and surrounding vasculature using localized light delivery and a photosensitizing drug. In contrast, low fluence rate PDT has recently been shown to increase permeability of vasculature to chemotherapy agents in several animal models by modifying the cell's cytoskeleton. This in turn leads to alteration in the endothelial cell shape, the loss of tight junctions, and ultimately an increase of vascular permeability [4–8]. Although the use of PDT to selectively enhance the distribution of macromolecular therapeutics to tumors is attractive, it remains a double-edged sword since it depends on optimal PDT conditions in order to avoid vasospasm, vessel thrombosis, and tissue infarction. In this chapter, several experimental light-based therapeutic modalities that could potentially be employed in the treatment of gliomas are reviewed.

11.2 Photochemical Internalization

Photochemical internalization (PCI) is a special type of PDT that can be used to enhance the delivery of macromolecules in a site-specific manner [9–14]. The concept is based on the use of specially designed photosensitizers, which localize preferentially in the membranes of endocytic vesicles. The photosensitizer, aluminum phthalocyanine disulfonate ($AlPcS_{2a}$), a phthalocyanine derivative containing two charged sulfonate groups linked to phthalic subunits in adjacent positions on the Pc molecule and an Al metal ion coordinated at its center (Fig. 11.1), is well suited for PCI. The most important and distinguishable property of $AlPcS_{2a}$ is its amphiphilicity which refers to chemical compounds possessing both hydrophilic

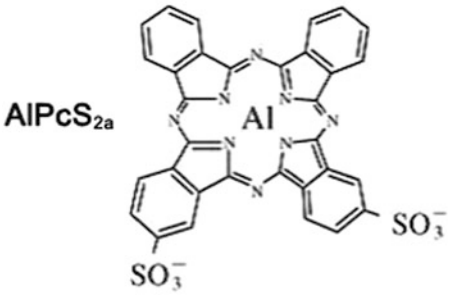

Fig. 11.1 Structure of the photosensitizer aluminum phthalocyanine dilsulphonate ($AlPcS_{2a}$)

and lipophilic properties. Most phthalocyanine photosensitizers are lipophilic and therefore insoluble in water, which makes them unsuitable for use in biological systems. This problem has been solved by sulfonation and by hydroxylation of the benzene rings in the phthalocyanine [15]. For example, while the phthalocyanine skeleton of $AlPcS_{2a}$ is lipophilic, the two adjacent sulfonate groups attached to the phthalocyanine molecule contribute to its hydrophilic nature. This amphiphilic photosensitizer is perfectly designed to localize in the cellular membrane [16]. This is achieved by inserting the lipophilic phthalocyanine skeleton of $AlPcS_{2a}$ in the lipophilic interior of the cellular membrane and dissolving the sulfonate groups in the hydrophilic outer layer of the membrane. $AlPcS_{2a}$ molecules first localize in the cell membrane. During endocytosis, a partial cell membrane with previously localized $AlPcS_{2a}$ molecules pinches inward to form an endocytic vesicle (endosome), and subsequently, the attached $AlPcS_{2a}$ molecules are transported into the cell via the endosomal membrane.

Although a number of small molecule drugs can readily enter cells, they have relatively low therapeutic specificity primarily due to their structural limitations. Since hydrophilic macromolecules are taken up by the cell body through endocytosis, they have to escape through the endosomal membrane into the cytosol in order to exert their full biological effects. Unfortunately, macromolecules are generally trapped in the endosome, and after endosome-lysosome fusion, are degraded by powerful lysosomal enzymes thereby losing their therapeutic effects.

Since the main target of PCI is the membranes of endocytic vesicles, the choice of membrane-localizing photosensitizer is important for effective PCI. In this respect, photosensitizers with an amphiphilic structure are the most efficient since the hydrophilic part of the photosensitizer prevents penetration through the cellular membrane. Once the photosensitizer is securely localized in the cell membrane, it will eventually be incorporated into the membranes of endocytic vesicles via the process of endocytosis. The photosensitizer must maintain its position within the endocytic vesicle, while the macromolecular drugs are trapped within the vesicle in order to avoid photochemical destruction of the macromolecules.

11.2.1 Mechanisms of PCI

While specific amphiphilic photosensitizers (e.g., $AlPcS_{2a}$) preferentially accumulate in the membranes of endosomes, upon light exposure the photosensitizer interacts with ambient oxygen to produce singlet oxygen. Since singlet oxygen has a very short range of action (< 20 nm), only the area of the vesicular membrane where the photosensitizer is localized will be damaged by singlet oxygen-mediated reactions with amino acids, unsaturated fatty acids, and cholesterol in the membrane bilayer. Although the exact structure of the damaged endosomes has not yet been elucidated, the results of vesicular membrane damage (either increased permeability or destructive opening depending on the light fluence and photosensitizer concentration) are easily demonstrated. The previously trapped macromolecular drugs can now be released from the endocytic vesicles into the cytosol in a fully functional form and are free to diffuse to their intended targets to exert their therapeutic effects. The PCI concept is illustrated in Fig. 11.2.

11.2.2 Advantages of PCI

PCI as a drug delivery technology has many advantages. (1) There are no restrictions on the size of the molecules that can be effectively delivered, making PCI highly suitable for a wide variety of molecules. (2) PCI also exhibits high site-specificity, which limits the biological effect to only illuminated areas and lowers the potential systemic side effects of the delivered drug. (3) PCI is a method that increases the therapeutic efficacy of a wide range of macromolecules allowing for the possibility of using lower drug doses to minimize morbidity. (4) PCI is well suited for combination with other modalities or strategies for targeted drug delivery, thus increasing the potential for further therapeutic improvements. PCI has also been shown to potentiate the biological activity of a large variety of macromolecules and other molecules that do not readily penetrate the plasma membrane, including proteins (e.g., protein toxins and immunotoxins), peptides, DNA delivered as a complex with cationic polymers or incorporated in adenovirus or adeno-associated virus, peptide-nucleic acids (PNA), and chemotherapeutic agents.

11.2.3 Blood Brain Barrier Opening

Localized opening of the BBB is a potentially useful application of both PDT and PCI as it could enhance the delivery of therapeutic agents for the treatment of a wide variety of brain diseases including cancer. Site-specific disruption of the BBB for drug delivery into the brain has been accomplished using a number of approaches including highly focused ultrasound [17] and laser-based techniques such as PDT

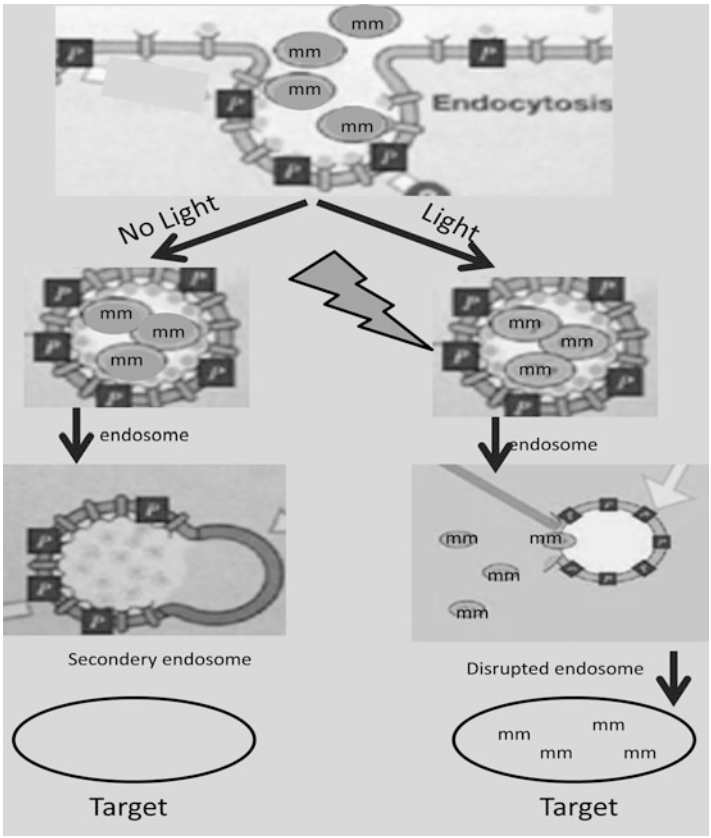

Fig. 11.2 Schematic illustration of PCI. Left panel; Macromolecules (mm) taken up through endocytosis and trapped in endosomes. Fusion with lysosomes (secondary endosomes) leads to their degradation before they have exerted their action. Right panel: PCI is based on accumulation of photosensitizer (PS) in endosomes. Light exposure causes rupture of the endo/lysosomal membrane and releases the mm into the cytosol where they can exert their biological activity

[18] and PCI [19].These approaches are appealing for a number of reasons including the highly localized nature of the BBB disruption: unlike the use of hyperosmolar solutions, the BBB is only disrupted at sites subjected to sufficient laser power densities which can be controlled by the user to coincide with the location of the pathology. Through judicious choice of beam parameters, the affected volume can be as small as a few mm^3. Equally important are observations showing that these highly focused approaches do not cause permanent damage to the BBB, as long as incident power densities remain below threshold levels. Under these conditions, the BBB may remain open for relatively long periods of time thus facilitating multi-fractionated drug delivery. In contrast, repeated injections of hyperosmotic compounds are required for extended treatment regimens since the BBB remains open for only a few minutes following bradykinin administration [20].

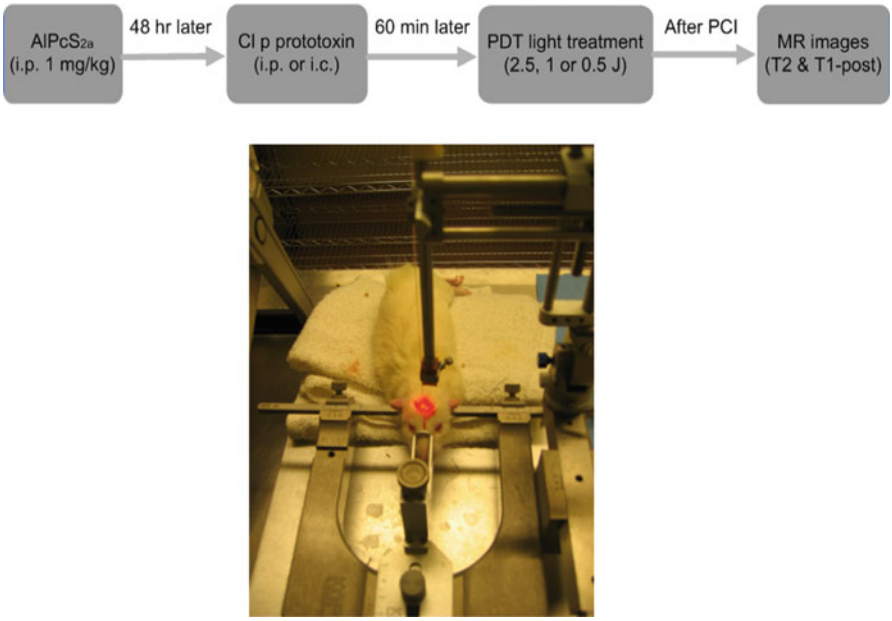

Fig. 11.3 Experimental protocol for Clp-PCI BBB disruption. Rats were fixed in the stereotactic frame and a skin incision was made exposing the skull. An optical fiber was placed in contact with the surface of the skull to the right of the midline. Surface light irradiation was given approximately 60 min after Clp ip administration

Localized BBB opening via PCI-mediated delivery of *Clostridium perfringens* epsilon prototoxin (Clp) was recently investigated in Fischer rats [19]. The rationale for using Clp is due to the ability of active toxin to cause widespread but reversible opening of the BBB [21–23]. Following systemic administration, Clp prototoxin is converted to fully active toxin by proteolytic cleavage. The experimental set up is shown in Fig. 11.3.

The results demonstrated that Clp-PCI was capable of causing localized BBB disruption at very low light fluences (1 J) as shown in Fig. 11.4.

Of particular interest was the time duration and evolution of the Clp-PCI BBB disruption since this represents the therapeutic window for drug delivery. Based on an analysis of MR images, enhancement volumes were observed to peak three days following Clp-PCI suggestive of maximum BBB opening at that time (Fig. 11.5). Thereafter, contrast volumes were observed to decrease, and by day 11, only trace amounts of contrast were observed.

In a follow-on study using an orthotopic brain tumor model consisting of F98 glioma cells in Fischer rats, newly implanted tumor cells were used to mimic the characteristics of infiltrating cells remaining in the resection margin usually found following surgical removal of bulk tumor. PDT or PCI localized BBB opening was performed 24 h after cell inoculation [24]. This is an insufficient time to allow for the development of bulk tumor and BBB degradation, but long enough for the cells

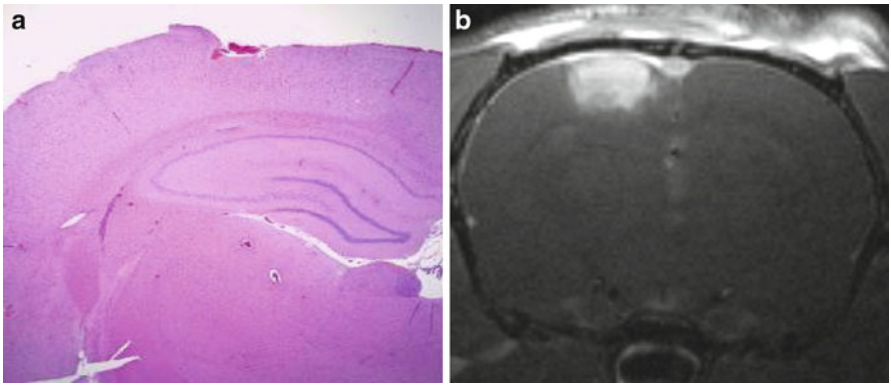

Fig. 11.4 Effects of Clp-PCI on BBB and tissue disruption. Coronal a: H&E sections from rat brains corresponding to T1 contrast MRI scans (b). The sections were taken 21 days post-treatment and the T1- weighted post-contrast images were acquired 3 days post-treatment

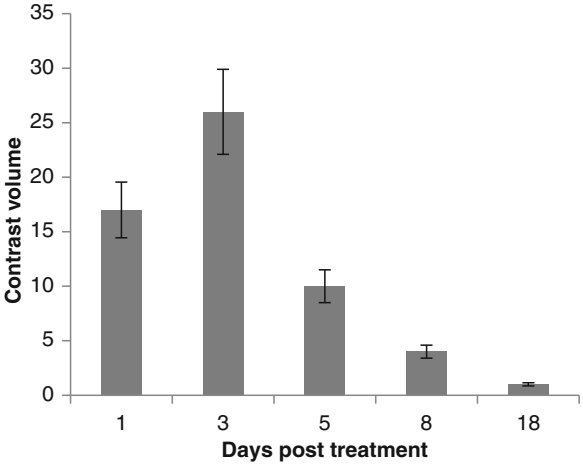

Fig. 11.5 Average time course of BBB opening induced by Clp-PCI. The animals (n = 4 per group) received i.p. injection of Clp at a concentration of 1:100, 1 mg kg^{-1} $AlPcS_{2a}$. and a light fluence of 1 J. Scanning was performed on days 1, 3, 5, 8 and 18 after treatment. All T1 post-contrast images were taken 15 min following i.p. contrast injection

(doubling time of approximately 18 h) to form small, sequestered, micro-clusters which are protected by an intact BBB. The survival of animals implanted with F98 tumor cells, as shown in Fig. 11.6, was significantly extended following BLM chemotherapy with PCI-mediated BBB opening compared to controls that received chemotherapy only.

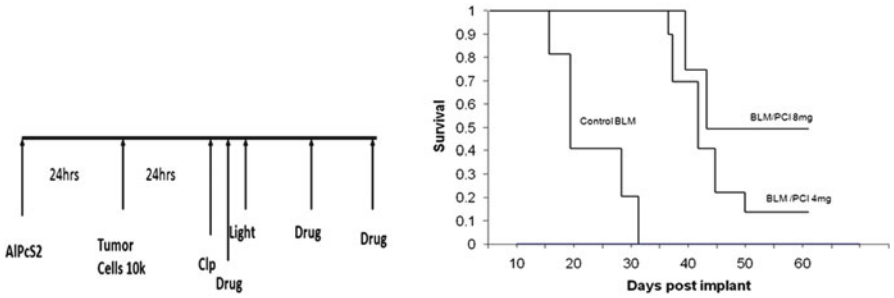

Fig. 11.6 Treatment protocol and Kaplan–Meier survival of tumor cell implanted animals. All animals received 1×10^4 cells i.c. Three groups were followed: BLM 8 mg/kg only, Clp-PCI BLM experimental groups ($AlPcS_{2a}$, Clp, 1 J); BLM 4 or 8 mg/kg was injected i.p. twice daily for 3 days

11.2.4 PCI-Mediated Drug Delivery

The limited efficacy of chemotherapy in the treatment of gliomas is caused by many factors, but two important ones are: (1) the blood brain barrier (BBB) which prevents chemotherapeutic agents from entering the brain and (2) limited endosomal escape of many drugs leading to their inactivation. Chemotherapeutics need to pass the blood brain barrier (BBB) and then enter into cells through the cell plasma membrane, which limits chemotherapeutic agents to mostly lipophilic or low molecular weight compounds that passively diffuse into the cell cytoplasm. In contrast, many highly effective chemotherapeutic agents are large and water-soluble and therefore do not easily penetrate plasma membranes but are actively transported into cells by endocytosis [25]. Their poor ability to escape from the resulting intracellular endosomes leads to their inactivation. Therefore, in combination with modalities leading to increased endosomal escape, the therapeutic effect of these agents would be significantly increased. As outlined above, we have previously shown that selective site-specific opening of the BBB could be obtained in the rat brain by the PCI-mediated potentiation of the effects of known BBB-disrupting agents [19]. BLM administered to animals with targeted BBB opening results in a significant increase in survival compared to drug-only controls. We have also examined the second factor limiting the efficacy of BLM chemotherapy, i.e., endosomal entrapment in in vitro experiments employing multicell tumor spheroids (MTS) formed from human gliomas cells. In comparison to monolayer cultures, a significant advantage of MTS is that their micro-environment more closely mimics the in vivo situation and therefore gene expression and the biological behavior of the cells are likely similar to that encountered in tumor cells in situ. The oxygen gradients characteristic of MTS produce a heterogeneous population of cells that differ in their response to oxygen-dependent therapies such as ionizing radiation, PDT, and chemotherapy. In addition to oxygenation status, tumor response to these therapies is controlled by a number of parameters including intercellular contact and

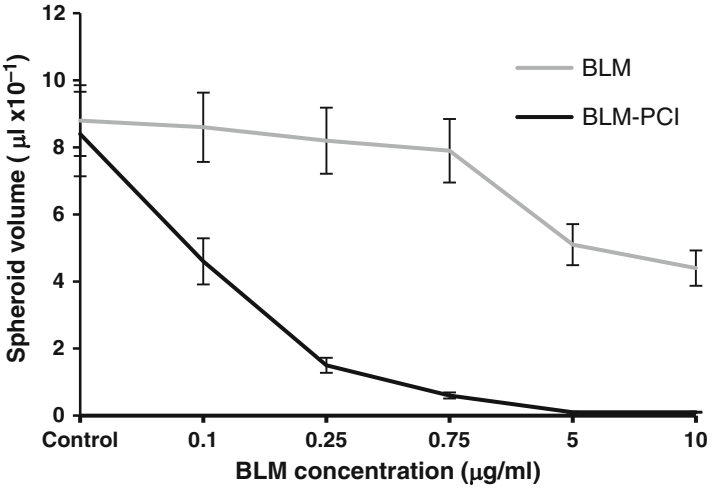

Fig. 11.7 Effects of BLM, and BLM PCI on human glioma MTS growth. Average spheroid volume measured following 4 weeks of incubation as a function of BLM concentration, 0.1–10 µg/mL. 1 µg/mL $AlPcS_{2a}$ incubation for 18 h. Wavelength of 670 nm: radiant exposure of 1.5 J/cm^2; irradiance of 5 mW/cm^2. Each data point represents the mean of 3 experiments. Error bars denote standard errors

communication and susceptibility to apoptosis. The anti-cancer agent bleomycin (BLM) was employed since the effects of BLM have been shown to be increased by PCI on a number of cell types, but its potential use for the treatment of gliomas has not been established [26]. The toxic effects on spheroid volume growth, evaluated after 4 weeks in culture, of PCI BLM were compared to the effects of BLM alone over a concentration range of 0.1–10 µg/mL (Fig. 11.7). As can be seen, PCI greatly enhanced the effects of the drug and the effects of PCI with 0.1 µg/mL BLM were equivalent to those observed at 10 µg/mL of drug alone.

The number of MTS showing growth after 3 weeks in culture out of a total of 24 replicate cultures in each group is shown in Fig. 11.8. These "survival" data can be used to ascertain if PCI is synergistic or simply additive compared to the results obtained for PDT or drug alone.

Synergism was calculated when analyzing PCI treatments. The equation shown was used to determine if the PCI effect was synergistic, antagonistic, or additive.

$$\alpha = \frac{SF^a \times SF^b}{SF^{ab}}$$

where a = PDT, b = BLM, and ab = PCI/BLM.

In this scheme SF represents the survival fraction for a specific treatment. If two treatments are to be compared, the survival fractions of each separate treatment are multiplied together and then divided by the survival fraction when both treatments

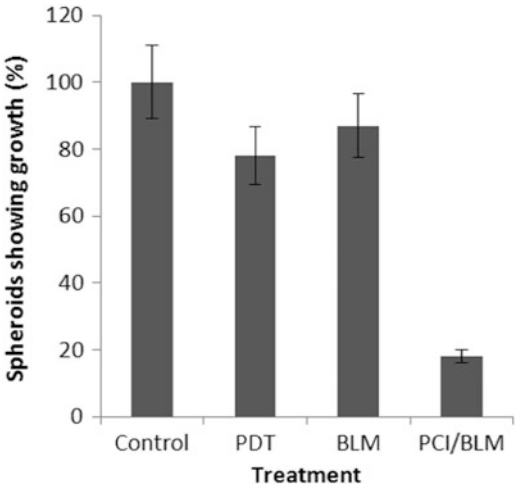

Fig. 11.8 Viability of control and treated human glioma MTS after 4 weeks in culture. 1 μg/mL $AlPcS_{2a}$ incubation for 18 h. Wavelength of 670 nm; radiant exposure of 1.5 J/cm^2, irradiance of 5 mW/cm^2, and 1-hour BLM incubation at a concentration of 0.25 μg/mL. Each data point represents the mean of 3 experiments. Error bars denote standard errors

were applied together. The resulting number (α) describes the cumulative effect. If $\alpha > 1$, the result is synergistic. If $\alpha < 1$, the result is antagonistic, and if $\alpha = 1$ the result is simply additive. The α value for the data shown in Fig. 11.8 was calculated to 3.8, a clearly synergistic effect.

11.2.5 Gene Therapy

Recent research has indicated that mutation or inactivation of tumor suppressor genes in normal neural stem cells (NSC), transforming them into tumor stem cells (TSC), is required and sufficient to induce malignant brain tumors [27]. NSC niches in the brain may harbor TSCs where targeted therapy can be directed [28]. The ability to insert functioning suppressor genes into tumor cells and TSCs would therefore be of considerable interest as a potential treatment modality. Although viral vectors have been used as gene carriers in clinical trials, nonviral vectors offer several advantages. These include flexibility for versatile design, large payloads of genes, and fewer safety concerns. In addition, nonviral vectors have the ability to circumvent the immune response (occurring against viral proteins) allowing iterative administration. One important limitation for cancer gene therapy though is the insurance that the therapeutic gene reaches a sufficient number of tumor cells in a high enough concentration to eliminate the tumor cells and at the same time leave the normal cells unaffected. Since macromolecules, such as DNA plasmids delivered as a complex with cationic polymers, are taken up by cells through endocytosis, they have to penetrate through the membranes of endosomes and into the cytosol in order to exert their full biological effects (see Fig. 11.2). The degradation of "trapped" macromolecules by powerful lysosomal enzymes following

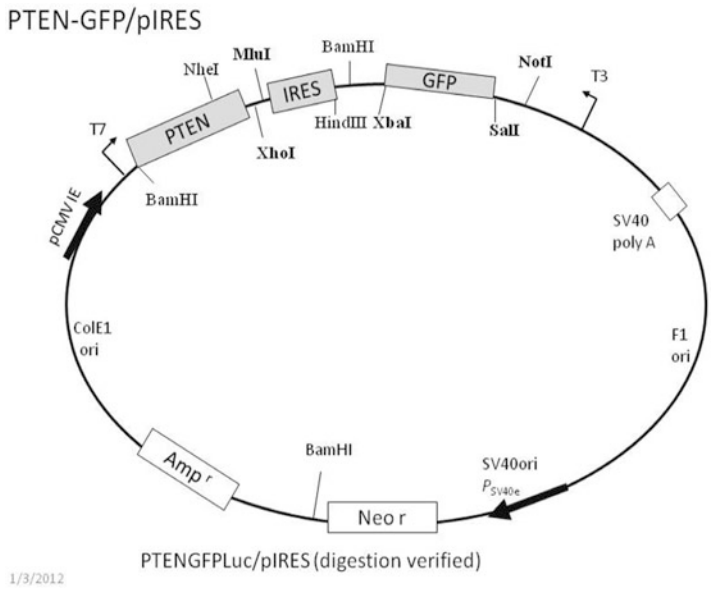

Fig. 11.9 Plasmid PTEN/GFP DNA construct

endosome–lysosome fusion remains a major limitation of gene therapy hindering its therapeutic potential. As previously mentioned, PCI has been shown to be a highly efficient technology for induced endolysosomal escape in a time and site-specific manner for gene therapy by enhanced delivery of various forms of RNA/DNA to the cytosol or nucleus of the targeted cells [29, 30].

PTEN is one of the most commonly lost tumor suppressors in human cancer [31]. Mutations and deletions of PTEN occur that inactivate its enzymatic activity leading to increased cell proliferation and reduced cell death. Frequent genetic inactivation of PTEN occurs in glioblastoma, endometrial cancer, and prostate cancer; and reduced expression is found in many other tumor types such as lung and breast cancer. The glioma cell line U251 MG is known to underexpress the PTEN gene product and can be used to determine the effects of transfection with a functioning PTEN gene. The utility of PCI for the delivery of the GFP indicator gene on the same plasmid as a tumor suppressor gene (PTEN) was investigated in monolayers of U251 human glioma cells. U251 monolayers were incubated in $AlPcS_{2a}$ for 18 h. together with the plasmid and nonviral vectors. In all cases, light treatment was performed with a diode laser at a wavelength of 670 nm. The nonviral transfection agents, branched PEI or protomine sulfate (PS), were used with the plasmid construct (GFP-PTEN: Fig. 11.9).

Since PCI is optimal with a light fluence level that allows 70–80% survival, we performed$AlPcS_{2a}$-mediated PDT at increasing light doses. Live/dead assay of U251 following PDT is shown in Fig. 11.10 for 0, 0.75 and 1.5 J, respectively. Fluence levels of 1.5 J cm^{-2} proved toxic killing more than 50% of the cells. Fluence levels of 0.5–0.75 J cm^{-2} seemed optimal.

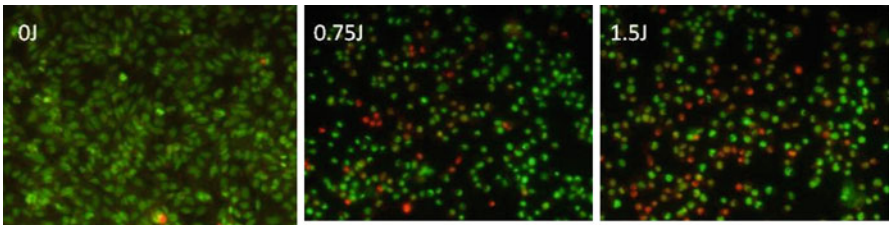

Fig. 11.10 Live-dead assay of U251 cell monolayers following $AlPcS_{2a}$ PDT. *Green* live, *red* dead

11.2.5.1 Effects of PCI on Protamine-Sulfate/DNA Polyplexes

We have investigated utilizing a GFP DNA - protamine-sulfate (PS) polyplex to transfect U251 glioma cells. The polyplexes enter the cell by endocytosis and are sequestered outside the nucleolus in endosomes, resulting in very low transfection rates (Fig. 11.11) [32]. The addition of PCI treatment demonstrated a tenfold increase in transfection rate at optimum PS/DNA concentrations. These results clearly demonstrate the ability of the PCI technique to greatly enhance endosomal escape.

U251 cell monolayers were transfected with the PTEN gene employing the gene carrier bPEI. As seen in Fig. 11.12, the introduction of this tumor suppressor gene inhibited cell growth. The growth inhibitory effect was significantly enhanced by PCI treatment.

These results demonstrate the ability of PCI to increase transfection rates in glioma cells as has been previously reported [33, 34]. Although bPEI is an effective gene carrier, it is highly toxic and is not well suited for in vivo applications. In contrast, PS is relatively non-toxic, but has relatively low transfection efficiency [35, 36]. PCI of PS/DNA polyplexes though could demonstrate a tenfold increase in transfection rate at optimum PS/DNA concentrations (Fig. 11.11). Nevertheless, PS polyplexes enter cells in similar amounts compared to PEI [32]. The difference in transfection efficiency between these two gene carriers is most probably due to increased endosomal escape by PEI/DNA polyplexes. Since PCI greatly enhances endosomal escape, the dramatic effects of PCI shown in Fig. 11.11 for PS/DNA polyplexes support this interpretation. Collectively, the results suggest that $AlPcS_{2a}$-mediated PCI can be used to enhance transfection of tumor suppressor genes in glioma cells or perhaps more importantly into transformed neuro stem cells [27, 28].

11.3 Photothermal Therapy (PTT)

The application of heat to destroy solid tumors (hyperthermia) has been used in cancer treatment for a variety of tumors. Sources for heat generation include microwaves, direct laser light, ultrasound, and near infrared activation of absorbing

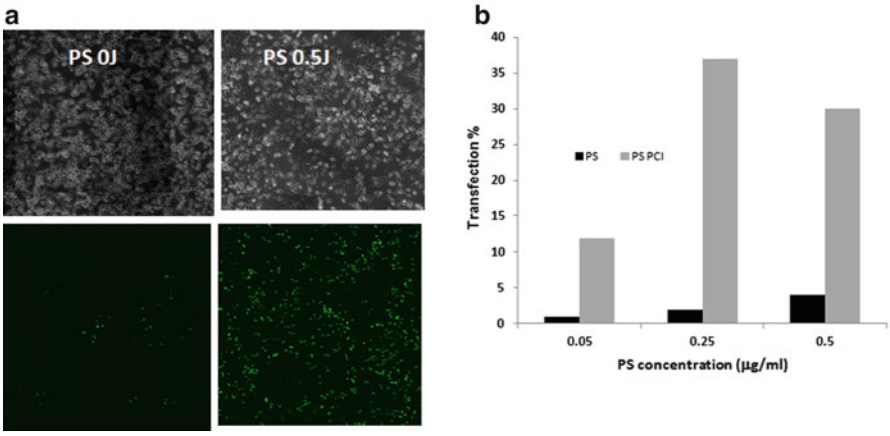

Fig. 11.11 Effects of PCI on GFP gene transfection with protamine-sulfate/DNA polyplexes. DNA complexed with protamine-sulfate, DNA concentration 1 µg mL^{-1}, PDT 0.75 J cm^{-2}. (**a**) Upper panels: phase contrast images showing cell densities; lower panels: two-photon fluorescence images, (**b**) % of cells expressing GFP

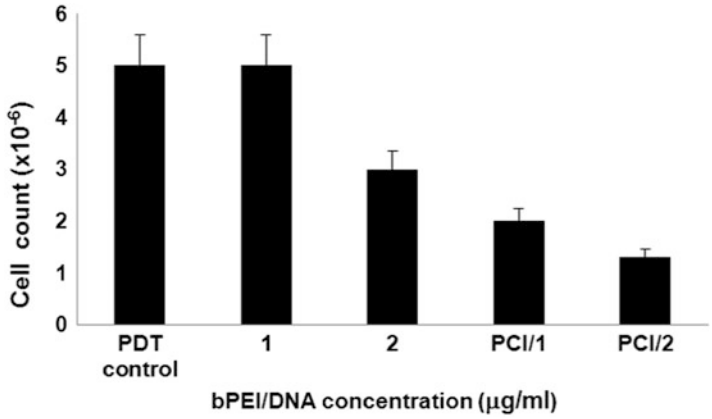

Fig. 11.12 U251 cell growth measured 48 h. following PTEN gene transfection. bPEI/DNA concentration 1 or 2 µg mL^{-1}, PDT 0.75 J cm^{-2}

agents. The latter, called photothermal therapy (PTT), will be discussed briefly in this portion of the chapter. A more detailed review of nanoparticle-mediated PTT can be found in Chap. 10. Unfortunately, the majority of hyperthermia techniques destroy both normal as well as diseased tissue limiting its usefulness. To overcome this limitation, nanoparticles can be used as exogenous energy absorbers to provide specific delivery of heat selectively to tumors. Particles delivered i.v. accumulate to a degree in the tumor by virtue of the enhanced permeability and retention effect (EPR) due to poorly organized and fenestrated vasculature as well as reduced lymphatic drainage [37, 38].

Nanoparticles are structures less than 500 nm in size which has sparked interest with their novel properties (optical, magnetic, and thermal). Gold nanoshells (NS) represent one class of photo-absorbing nanoparticles [39, 40]. They consist of a spherical dielectric silica core (50–500 nm) surrounded by a thin (5–20 nm) gold layer and have a tunable optical absorption within the visible and infrared regions. Since nanoshells are roughly one million times more efficient at converting NIR light into heat than conventional dyes such as indocyanine green, once localized to the tumor and exposed to NIR light, they can generate sufficient heat to induce cell death by mechanisms such as protein denaturation and rupture of cellular membranes via thermal ablation**.**

As gliomas grow, their centers are largely necrotic, due to the rapid proliferation of malignant cells within the core of the tumor at increasingly larger distances from their nearest capillaries. Although this isolation of cells renders the hypoxic areas of gliomas inaccessible to nanoparticle-based therapies where delivery into the tumor is based on the EPR effect, this portion of the tumor is resected during surgery. It is in the resection margins, partially protected by the blood brain barrier, that it is desirable for the nanoparticles to accumulate. Since the vasculature in this region can be more or less normal, the EPR effect will be insufficient to allow the concentration of nanoshells, necessary for hyperthermia, to be reached. One method to overcome this limitation would be to use cells such as stem cells or macrophages to act as vectors.

Tumor-associated macrophages (TAMs) are frequently found in and around glioblastomas in both experimental animals and patient biopsies [41, 42]. This would indicate local synthesis of chemo attractive factors in gliomas and that inflammatory cells can pass through an intact BBB. Monocyte trafficking into the CNS occurs in a highly regulated fashion and is dependent on cell–cell interactions that involve endothelial cells and astrocytes, as well as the local release of factors that promote BBB permeability. Intravenously injected macrophages loaded with iron oxide nanoparticles have been shown to target experimental brain tumors [43]. This would indicate local synthesis of chemo attractive factors in gliomas and that inflammatory cells can pass through an intact BBB. Monocytes or macrophages loaded with drugs, nanoparticles, or photosensitizers could therefore be used to target tumors [44]. The use of macrophages loaded with gold nanoshells for thermal ablation of GBM tumors is potentionally an attractive, relatively safe treatment modality that is worth studying.

We have investigated the effects of exposure to laser NIR in vitro on multicell human glioma spheroids infiltrated with empty (containing no nanoshells) or nanoshell-loaded macrophages [45, 46]. The gold nanoshells (NS) used in this study consisted of a 120 nm silica core with a 12–15 nm gold shell (Nanospectra Biosciences, Inc., Houston, Texas). The resultant optical absorption peak was between 790 and 820 nm for both bare and PEGylated particles. PEGylated nanoshell solutions as supplied by the manufacturer are shown in Fig 11.13.

Gold nanoshells are often PEGylated to prevent their rapid uptake and removal from circulation by the reticulo-endothelial system. The % uptake of PEGylated nanoshells in murine macrophages was lower (3.96%) than that of bare nanoshells

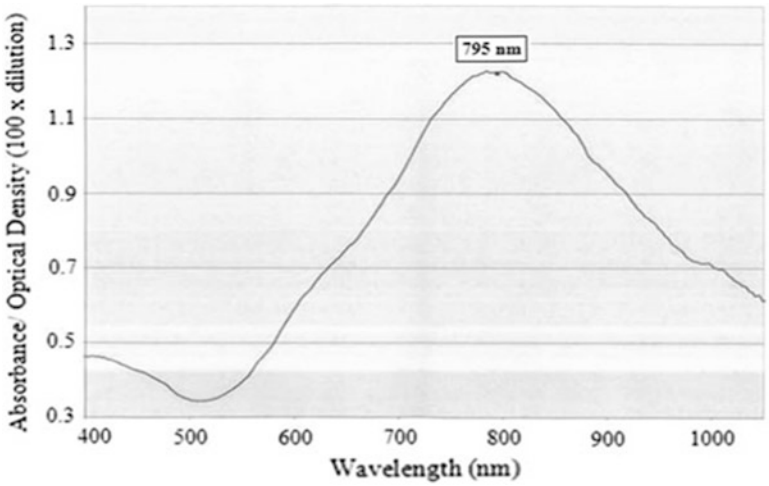

Fig. 11.13 Absorbance curves of PEGylated nanoshell solutions

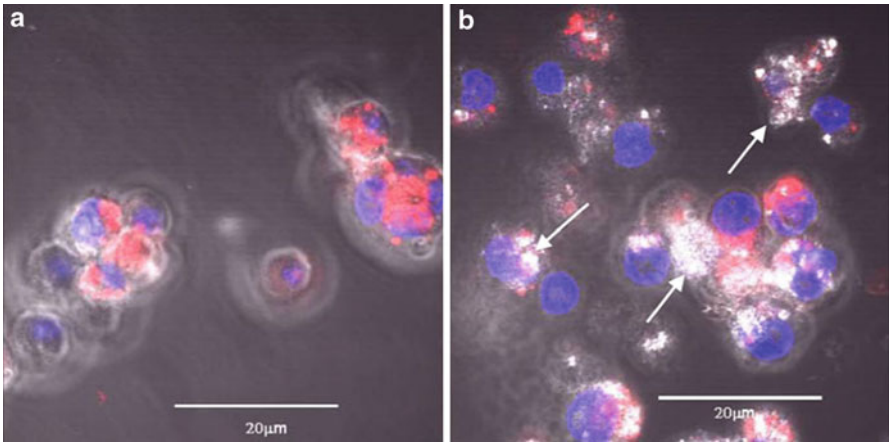

Fig. 11.14 Two-photon fluorescence micrograph of (**a**) empty or (**b**) nanoshell-loaded Ma. Cell nucleus stained with Hoechst 33342 (*blue*), Cytoplasm stained with PKH26 Red Fluorescent (*red*), nanoshell aggregates inside Ma shown by white reflectance (*white arrows*)

(15.74%). However, the PEGylated nanoshell solution was available in a much higher concentration since they have a much lower tendency to aggregate compared to bare nanoshells. Comparison was therefore between the respective numbers of nanoshells taken up by a given number of macrophages. The total amount of PEGylated nanoshells taken up by the macrophages was more than eight times that of bare nanoshells. As seen in Fig. 11.14, macrophages could efficiently take up PEGylated gold NS

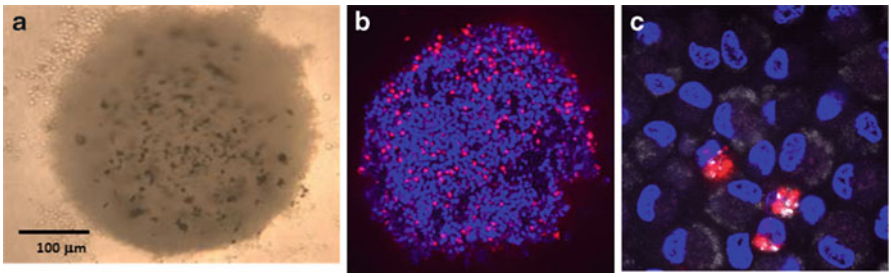

Fig. 11.15 Light and two-photon micrographs of 48 h co-culture of human tumor spheroid and NS-loaded labeled Ma. The Ma (*red*) are seen to migrate throughout the tumor cells (*blue*) making up the spheroid. (**a**) Light microscope ×10, (**b**) two photon ×10, (**c**) two photon ×40

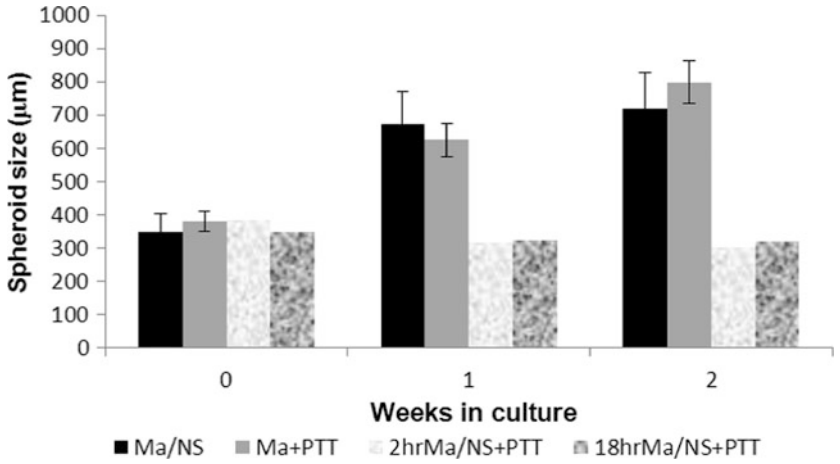

Fig. 11.16 Kinetics of spheroid growth following PTT. Spheroids were formed containing 5×10^3 tumor cells. 48 h after formation, individual spheroids were co-incubated with 2×10^4 empty Ma or NS-loaded Ma for 2 or 18 h. PTT: 14 W cm^{-2}, 10 min. Ma/NS: nanoshell-loaded macrophages—no PTT; Ma +PTT: empty macrophages +PTT

The ability of NS-loaded Ma to infiltrate into multicellular tumor spheroids is clearly illustrated in Fig. 11.15. The monocytes were labeled with a red fluorescent dye and are shown in Fig. 11.15 at two magnifications developed by two-photon microscopy. Mo/Ma were seen to be distributed through the spheroid. This is most probably caused by chemoatractive agents produced by the tumor cells acting on the Ma. NS-loaded macrophages infiltrated into glioma spheroids to the same or, in some cases, to a greater degree than empty Ma [45].

NIR laser irradiation of spheroids incorporating NS-loaded macrophages resulted in complete growth inhibition in an irradiance-dependent manner, while spheroids infiltrated with empty macrophages had growth curves identical to untreated controls following PTT treatment (Fig. 11.16).

11.4 Conclusions

Tumor resection is usually the first modality employed in the treatment of gliomas. With the improved surgical techniques now available, the incidence of gross tumor resection, as defined by a negative post operative MRI, has greatly increased [47, 48]. Nevertheless, the great majority of glioma patients do suffer a recurrence of their tumors leading to their poor prognosis. The therapeutic goal following surgical resection therefore is the elimination of infiltrating tumor cells remaining in the margins of the resection cavity, where most tumors recur, while minimizing damage to normal brain. One of the many obstacles to effective treatment of malignant brain tumors is limited transport of anti-tumor agents through both brain and brain tumor capillaries due to the BBB and the blood–brain tumor barrier (BBTB), the latter which retains many BBB characteristics. We have explored a number of methods, as described in this chapter, for enhancing both drug delivery and efficacy across the BBB and into tumors. Additionally, the ability of macrophages to migrate and accumulate within, and at the periphery, of brain tumors renders them attractive vehicles for the delivery of anti-tumor agents including nanoparticles.

In a clinical setting, light delivered directly into the wall of the tumor resection cavity is required for PCI, PDT, and PTT. Laser light applied through an indwelling balloon applicator filling the resection cavity could meet this requirement [49, 50].

References

1. Wallner KE, Galicich JH, Krol G, Arbit E, Malkin MG (1989) Patterns of failure following treatment for glioblastoma multiforme and anaplastic astrocytoma. Int J Radiat Oncol Biol Phys 16:1405–9
2. Brem H, Piantadosi S, Burger PC et al (1995) Placebo-controlled trial of safety and efficacy of intraoperative controlled delivery by biodegradable polymers of chemotherapy for recurrent gliomas. Lancet 345(8956):1008–12
3. Johannesen TB, Watne K, Lote K, Norum J, Tvera K, Hirschberg H (1999) Intracavity fractionated balloon brachytherapy in glioblastoma. Acta Neurochir 141:127–33
4. Boekelheide K, Eveleth J, Tatum A, Winkelman J (1987) Microtubule assembly inhibition by porphyrins and related-compounds. Photochem Photobiol 46:657–661
5. Dadosh N, Shaklai N (1987) Effect of protoporphyrin-IX on red blood-cell membrane cytoskeleton. J Muscle Res Cell Motil 9:86–92
6. Nelson J, Liaw L, Berns M (1987) Tumor destruction in photodynamic therapy. Photochem Photobiol 46:829–835
7. Sporn L, Foster T (1992) Photofrin and light induces microtubule depolymerization in cultured human endothelial-cells. Cancer Res 52:3443–3448
8. Chen B, Pogue BW, Luna JM et al (2006) Tumor vascular permeabilization by vascular-targeting photosensitization: effects, mechanism, and therapeutic implications. Clin Cancer Res 12:917–923
9. Berg K, Selbo PK, Prasmickaite L et al (1999) Photochemical internalization: a novel technology for delivery of macromolecules into cytosol. Cancer Res 59(6):1180–83

10. Dietze A, Peng Q, Selbo PK et al (2005) Enhanced photodynamic destruction of a transplantable fibrosarcoma using photochemical internalization of gelonin. Br J Cancer 92:2004–9
11. Selbo PK, Kaalhus O, Sivam G, Berg K (2001) 5- aminolevulinic acid-based photochemical internalization of the immunotoxin MOC31-gelonin generates synergistic cytotoxic effects in vitro. Photochem Photobiol 74:303–10
12. Selbo PK, Sivam G, Fodstad Ø, Sandvig K, Berg K (2000) Photochemical internalization increases the cytotoxic effect of the immunotoxin MOC31 gelonin. Int J Cancer 87:853–9
13. Prasmickaite L, Høgset A, Selbo PK et al (2002) Photochemical disruption of endocytic vesicles before delivery of drugs: a new strategy for cancer therapy. Br J Cancer 86:652–7
14. Selbo PK, Weyergang A, Høgset A et al (2010) Photochemical internalization provides time- and space-controlled endolysosomal escape of therapeutic molecules. J Control Release 148(1):2–12
15. Berg K, Bommer J, Moan J (1989) Evaluation of sulfonated aluminum phthalocyanines for use in photochemotherapy. Cellular uptake studies. Cancer Lett 44:7–15
16. Maman N, Dhami S, Phillips D, Brault D (1999) Kinetic and equilibrium studies of incorporation of di-sulfonated aluminum phthalocyanine into unilamellar vesicles. Biochim Biophys Acta 1420:168–178
17. Vykhodtseva N, McDannold N, Hynynen K (2008) Progress and problems in the application of focused ultrasound for blood–brain barrier disruption. Ultrasonics 48:279–96
18. Hirschberg H, Uzal FA, Chighvinadze D, Zhang MJ, Peng Q, Madsen SJ (2008) Disruption of the blood–brain barrier following ALA-mediated photodynamic therapy. Lasers Surg Med 40:535–41
19. Hirschberg H, Zhang MJ, Gach HM et al (2009) Targeted delivery of bleomycin to the brain using photo-chemical internalization of Clostridium perfringens epsilon prototoxin. J Neurooncol 95(3):317–29
20. Murphy LJ, Hachey DL, Oates JA et al (2000) Metabolism of bradykinin in vivo in humans: identification of BK1-5 as a stable plasma peptide metabolite. J Pharmacol Exp Ther 294 (1):263–9
21. Worthington R, Mulders M (1975) The effect of Clostridium perfringens epsilon toxin on the blood–brain barrier of mice. Onderstepoort J Vet Res 42:25–31
22. Nagahama M, Sakurai J (1991) Distribution of labeled Clostridium perfringens epsilon toxin in mice. Toxicon 29:211–7
23. Dorca-Arevalo J, Soler-Jover A, Gibert M et al (2008) Binding of epsilon toxin from Clostridium perfringens in the nervous system. Vet Microbiol 131:14–20
24. Madsen SJ, Angell-Petersen E, Spetalen S, Carper SW, Ziegler SA, Hirschberg H (2006) Photodynamic therapy of newly implanted glioma cells in the rat brain. Lasers Surg Med 38:540–548
25. Pron G, Mahrour N, Orlowski S (1999) Internalization of the bleomycin molecules responsible for bleomycin toxicity: a receptor-mediated endocytosis mechanism. Biochem Pharmacol 57:45–56
26. Berg K, Dietze A, Kaalhus O, Hogset A (2005) Site-specific drug delivery by photochemical internalization enhances the antitumor effect of bleomycin. Clin Cancer Res 11(23):8476–85
27. Alcantara L, Laguno S et al (2009) Malignant astrocytomas originate from neural stem/progenitor cells in a somatic tumor suppressor mouse model. Cancer Cell 15(1):45–56
28. Evers P, Lee PP et al (2010) Irradiation of the potential cancer stem cell niches in the adult brain improves progression free survival of patients with malignant gliomas. BMC Cancer 10:384–9
29. Hogset A, Ovstebo Engesaeter B, Prasmickaite L et al (2002) Light induced adenovirus gene transfer, an efficient and specific gene delivery technology for cancer gene therapy. Cancer Gene Ther 9:365–371
30. Ndoye A, Dolivet G, Hogset A et al (2006) Eradication of p53-mutated head and neck squamous cell carcinoma xenografts using nonviral p53 gene therapy and photochemical internalization. Mol Ther 13(6):1156–62

31. Knobbe CB, Merlo A, Reifenberger G (2002) Pten signaling in gliomas. Neuro Oncol 4(3):196–211
32. Cho SK, Kwon YJ (2011) Polyamine/DNA polyplexes with acid-degradable polymeric shell as structurally and functionally virus-mimicking nonviral vectors. J Control Release 150:287–297
33. Chou CH, Sun CH, Zhou YH, Madsen SJ and Hirschberg H (2011) Enhanced transfection of brain tumor suppressor genes by photochemical internalization. Proceedings SPIE, photonic therapeutics and diagnostics, vol 7883, p 3U
34. Hirschberg H, Mathews MB, Shih EC, Madsen SJ, Kwon YJ (2012) Enhanced gene transfection by photochemical internalization of protomine sulfate/DNA complexes. Proceedings SPIE, Photonic therapeutics and diagnostics, vol 8207, p S1
35. Tsuchiya Y, Ishti T, Okahata Y, Sato T (2006) Characterization of protamine as a transfection accelerator for gene delivery. J Bioact Compat Polym 21:519–537
36. Liu J, Guo S, Li Z, Liu L, Gu J (2009) Synthesis and characterization of stearyl protamine and investigation of their complexes with DNA for gene delivery. Colloids Surf B Biointerfaces 73(1):36–41
37. Maeda H (2001) The enhanced permeability and retention (EPR) effect in tumor vasculature: the key role of tumor-selective macromolecular drug targeting. Adv Enzyme Regul 41:189–207
38. Maeda H, Fang J, Inutsuka T, Kitamoto Y (2003) Vascular permeability enhancement in solid tumor: various factors, mechanisms involved and its implications. Int Immunopharmacol 3:319–328
39. Huang X, Qian W, El-Sayed IH, El-Sayed MA (2007) The potential use of the enhanced nonlinear properties of gold nanospheres in photothermal cancer therapy. Lasers Surg Med 39(9):747–753
40. Schwartz JA, Shetty AM, Price RE, Stafford RJ, Wang JC, Uthamanthil RK et al (2009) Feasibility study of particle-assisted laser ablation of brain tumors in orthotopic canine model. Cancer Res 69(4):1659–1667
41. Badie B, Schartner JM (2000) Flow cytometric characterization of tumor associated macrophages in experimental gliomas. Neurosurgery 46:957–61 discussion 61–2
42. Roggendorf W, Strupp S, Paulus W (1996) Distribution and characterization of microglia/macrophages in human brain tumors. Acta Neuropathol 92:288–93
43. Valable S, Barbier EL, Bernaudin M, Roussel S, Segebarth C, Petit E et al (2008) In vivo MRI tracking of exogenous monocytes/macrophages targeting brain tumors in a rat model of glioma. Neuroimage 40(2):973–983
44. Choi MR, Stanton-Maxey KJ, Stanley JK et al (2007) A cellular Trojan Horse for delivery of therapeutic nanoparticles into tumors. Nano Lett 7(12):3759–3765
45. Baek SK, Makkouk AR, Krasieva T, Sun CH, Madsen SJ, Hirschberg H (2011) Photothermal treatment of glioma; an in vitro study of macrophage-mediated delivery of gold nanoshells. J Neurooncol 104(2):439–48
46. Madsen SJ, Baek SK, Makkouk AK, Krasieva T, Hirschberg H (2012) Macrophages as cell-based delivery systems for nanoshells in photothermal therapy. Ann Biomed Eng 40 (2):507–15
47. Hirschberg H, Samset E, Hole PK, Lote K (2006) Impact of intraoperative MRI on the results of surgery for high grade gliomas. J Min Inv Neurosurg 48:77–84
48. Stummer W, Pichlmeier U, Meinel T, Wiestler OD, Zanella F, Reulen HJ (2006) Fluorescence-guided surgery with 5-aminolevulinic acid for resection of malignant glioma: a randomized controlled multicentre phase III trial. Lancet Oncol 7:392–401
49. Madsen SJ, Sun CH, Tromberg BJ, Hirschberg H (2001) Development of a novel balloon applicator for optimizing light delivery in photodynamic therapy. Lasers Surg Med 29:406–10
50. Madsen SJ, Svaasand LO, Tromberg BJ, Hirschberg H (2001) Characterization of optical and thermal distributions from an intracranial balloon applicator for photodynamic therapy. Proc SPIE 4257:41